Bioinspir. Biomim. **8** (2013) 016005 (12pp) doi:10.1088/1748-3182/8/1/016005

Swimming near the substrate: a simple robotic model of stingray locomotion

Erin Blevins[1] **and George V Lauder**

The Museum of Comparative Zoology, 26 Oxford St., Harvard University, Cambridge, MA, USA

E-mail: eblevins@fas.harvard.edu

Received 15 June 2012
Accepted for publication 23 October 2012
Published 15 January 2013
Online at stacks.iop.org/BB/8/016005

Abstract
Studies of aquatic locomotion typically assume that organisms move through unbounded fluid. However, benthic fishes swim close to the substrate and will experience significant ground effects, which will be greatest for fishes with wide spans such as benthic batoids and flatfishes. Ground effects on fixed-wing flight are well understood, but these models are insufficient to describe the dynamic interactions between substrates and undulating, oscillating fish. Live fish alter their swimming behavior in ground effect, complicating comparisons of near-ground and freestream swimming performance. In this study, a simple, stingray-inspired physical model offers insights into ground effects on undulatory swimmers, contrasting the self-propelled swimming speed, power requirements, and hydrodynamics of fins swimming with fixed kinematics near and far from a solid boundary. Contrary to findings for gliding birds and other fixed-wing fliers, ground effect does not necessarily enhance the performance of undulating fins. Under most kinematic conditions, fins do not swim faster in ground effect, power requirements increase, and the cost of transport can increase by up to 10%. The influence of ground effect varies with kinematics, suggesting that benthic fish might modulate their swimming behavior to minimize locomotor penalties and incur benefits from swimming near a substrate.

(Some figures may appear in colour only in the online journal)

1. Introduction

Benthic fish are specialized for life at the boundary between fluid and solid environments. Many species use the substrate for a direct boost to propulsion: various forms of fin-walking are seen across benthic taxa from lungfish (King *et al* 2011), to skates and rays (Lucifora and Vassallo 2002, Koester and Spirito 2003, Macesic and Kajiura 2010), sharks (Pridmore 1994, Goto *et al* 1999, Wilga and Lauder 2001), and many teleosts (e.g. frogfish, Pietch and Grobecker 1987; flying gurnards, Renous *et al* 2000; and batfish, Ward 2002). However, even without direct contact, locomotion is influenced—and can be enhanced—by a nearby substrate, as ground effects alter fluid flow in the narrow gap between substrate and fish (Blake 1979, Webb 1981, 1993, 2002, Nowroozi *et al* 2009).

Ground effects are most commonly considered for rigid, static structures, in many computational and experimental studies of fixed-wing airfoils. In general, ground effects are greatest on broad structures moving close to the ground, as the magnitude of ground effect depends on the ratio of gap (the distance between the structure and the ground) to span (the width of the structure parallel to the ground) (Reid 1932). Ground effects decrease rapidly as the gap/span ratio increases, becoming negligible at a ratio of 3 (Reid 1932, Blake 1979, 1983). The consequences of moving near the ground vary substantially with foil shape (e.g. planform, camber, angle of attack) and distance from the substrate (Zerihan and Zhang 2000, Zhang *et al* 2004, Ahmed and Sharma 2005). However, human designs such as wing-in-ground aircraft (built for flight very near the ground; Rozhdestvendky 2006) and biological fixed-wing fliers can both experience significant gains in locomotor performance due to ground effect. The presence of a nearby substrate reduces flight costs in gliding birds

[1] Auhor to whom any correspondence should be addressed.

Table 1. Gap/span ratios and wavespeeds of undulating model fins swimming near and far from a solid wall, under all tested kinematic conditions ($n = 15$ for single-attachment fin conditions, $n = 10$ for double-attachment fin conditions). Values from stingrays swimming in midwater are given for comparison.

Fin Type	Kinematics	Gap/Span[a]		Wavespeed (c) (cm s^{-1})	
(Attachment No.)	(Frequency, Amplitude)	Center	Wall	Center	Wall
Single	1 Hz, 1 cm	1.5	0.4	7.8	7.0
Single	1 Hz, 2 cm	1.6	0.4	14.8	16.4
Single	2 Hz, 1 cm	1.5	0.4	21.7	18.5
Single	2 Hz, 2 cm	1.7	0.6	25.0	26.5
Double	1 Hz, 1 and 2 cm	1.5	0.4	14.4	18.1
Double	2 Hz, 1 and 2 cm	1.7	0.5	55.6	61.4
Stingray[b]	2.5 Hz, 1.4 cm	~1.0	–	31.0	–
Stingray[c]	3.8 Hz, 1.4 cm	~1.0	–	46.0	–

[a]As the ratio of gap (distance between structure and wall) to span (width of structure parallel to wall) decreases, the influence of ground effect increases, with significant effects occurring when gap/span <1 (Webb 1993).
[b, c] From Blevins and Lauder (2012) for freshwater stingray *Potamotrygon orbignyi* swimming at (a) 20 cm s^{-1} and (b) 33 cm s^{-1}.

(Baudinette and Schmidt-Nielsen 1974, Withers and Timko 1977, Hainsworth 1988) and increases glide distance in flying fish (Park and Choi 2010).

Performance benefits from locomotion in ground effect are significant for engineers and organisms alike, with the potential for large reductions in cost of transport (15%) and power requirements (35%) (Rayner 1991). However, fixed-wing models are insufficient to describe the ground effects experienced by most organisms, or in biomimetic designs. Very few models consider ground effects on moving foils (Tanida 2001, Argentina *et al* 2007, Molina and Zhang 2011), yet in the vast majority of cases, animal locomotion is dynamic—wings, fins, and bodies flex and flap over time. When an animal moves near the ground (a substrate, wall, etc), these locomotor motions continuously alter the animal's distance from the substrate and its effective shape. The pressure and flow structure between the animal and the substrate will fluctuate as well, creating a dynamic ground effect that varies during locomotion.

Fish swim by oscillating and undulating the body and fins, and are therefore subject to dynamic ground effects when swimming near a solid boundary. Most fish (e.g. trout, bluegill sunfish) are laterally compressed and swim 'upright;' due to their very narrow ventral span, they are unlikely to experience significant ground effects from swimming near the substrate (high gap/span ratio; Webb 2002). However, these fish can experience wall effects (analogous to ground effects) when swimming near the solid side wall of a channel; the gap/span ratio will decrease as the broad lateral surface of the body and caudal fin approaches the wall, with significant effects at gap/span <1 (Webb 1993). In contrast, many benthic fish species are compressed in the same plane as the substrate—the most notable and extreme examples are the flatfishes (*Pleuronectiformes*) and stingrays (here referring to benthic, undulatory members of *Batoidea*). These fishes undulate in close proximity to the substrate with a low gap/span ratio, and are likely to experience significant ground effect. Undulatory locomotion, whether by a stingray, eel, or flatfish, produces strong lateral jets (Webb 2002, Tytell and Lauder 2004), with great potential to alter the pressure and flow between fish and wall or ground. Plaice alter their kinematics as they swim closer to the substrate, suggesting a response to ground effect (Webb 2002). However, studies of live fish do not allow the kinematic manipulations or force measurements required for a detailed investigation of ground effects on undulatory swimming performance.

In this study, a simple physical model inspired by the swimming of freshwater stingray *Potamotrygon orbignyi* (Castelnau 1855) is used to examine the effects of a nearby substrate on undulatory swimmers. Rather than creating a complex biomimetic stingray, the aim of this investigation is to approximate the flow conditions experienced by broad-bodied swimmers undulating near a substrate, using a simple robotic system in which motion parameters can be easily altered, input forces measured, and consistent kinematics maintained during swimming near and far from a solid boundary (in and out of ground effect). The dimensions and motion parameters of the model fin were selected to correspond with stingray kinematics determined in previous work on pectoral fin locomotion by *P. orbignyi* (Blevins and Lauder 2012); fin width, length, and the range of undulation frequency, amplitude, wavespeed and swimming speed encompass values determined for live stingrays (figure 1). Therefore, three main indicators of fluid regime and flow structure, Reynolds number (~10 000), Strouhal number (~0.2), and slip (wavespeed/swimming speed, ~0.6) are similar for model fins and stingrays. Self-propelled swimming speeds, costs-of-transport, and hydrodynamics are determined for undulating fins swimming in and out of ground effect. Comparisons are made between identical fins swimming with identical kinematics in one of two positions, either in the center of a recirculating flow tank ('center position') or near the sidewall of the tank ('wall position'). As model fins swim parallel to the tank wall, with the undulatory wave occurring perpendicular to the wall (figure 2), this situation is analogous to a stingray undulating near the substrate: in the wall position, fins swim in ground effect (gap/span <1, table 1). Two fin structures (described in detail below) are tested under various combinations of frequency (1 and 2 Hz) and undulation amplitude (1–2 cm). This experimental study of ground

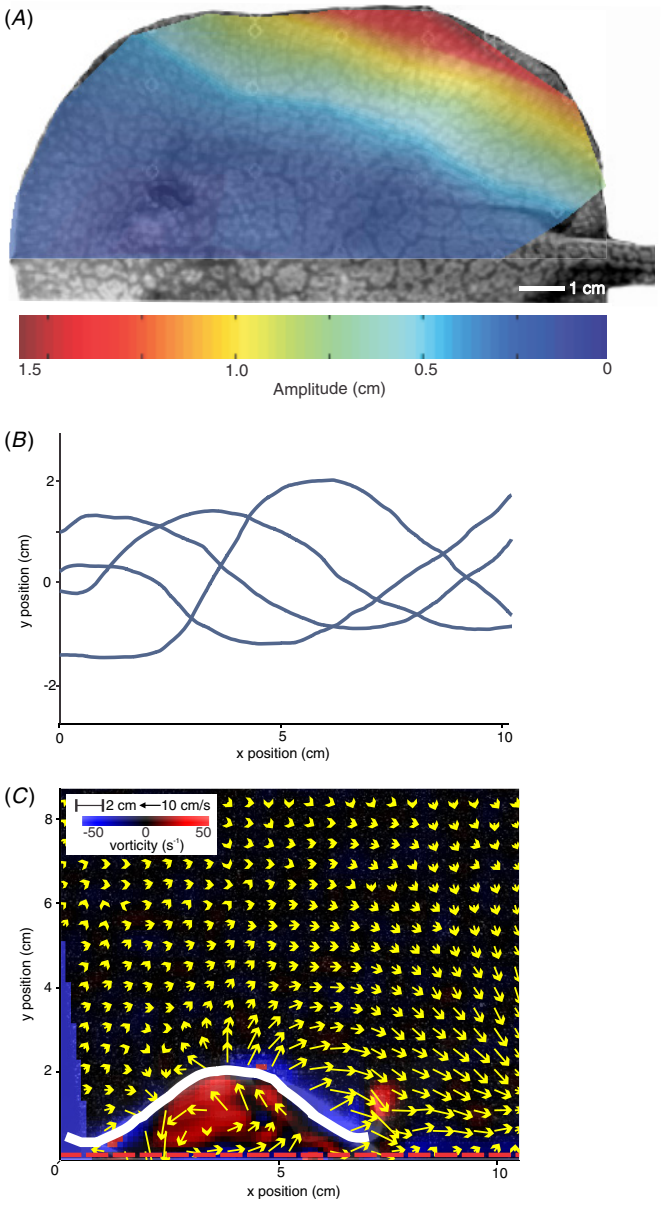

Figure 1. (*A*) Amplitude variation overlaid across the surface of the pectoral fin of freshwater stingray *Potamotrygon orbignyi* during steady swimming, with warmer colors indicating greater amplitude (from Blevins and Lauder 2012). Amplitude values represent 1/2 of the maximum excursion occurring at each point during one wave cycle. (*B*) Traces of the distal edge of the stingray pectoral fin (posterior quadrant) during locomotion near the substrate, at 25%, 50%, 75% and 100% of a wave cycle (compare to midline traces of the model fin in figure 3). Anterior is at left. Pectoral fin amplitude is slightly greater than shown in (*A*), where stingrays were swimming steadily in midwater. (*C*) Hydrodynamic analysis of flow around the undulating stingray pectoral fin (highlighted in white) during locomotion near the substrate, illustrating vortex compression between fin and ground. Anterior is at left. Yellow vector arrows represent flow speed and direction relative to freestream flow, with vorticity indicated by red (positive) and blue (negative) shading. For clarity, only 1/4 of vectors are shown. Vectors were not computed for masked areas (bright blue) outside the laser light sheet and overlapping the ground. See online publication for color images.

effects on an undulating model offers insight into the likely consequences of swimming near the substrate for stingrays and other benthic undulators.

2. Methods

A simple model system was used to investigate the influence of ground effect on undulatory swimmers: a flexible fin (30 Shore A Neoprene, 15 × 7.5 × 0.3 cm^3) connected to a robotic apparatus controlling the heave and pitch of the fin through time. (For a detailed description of the control apparatus, see Lauder *et al* 2007, 2011a, 2011b, and Alben *et al* 2012). The heave and pitch motors driving the fin are controlled by a custom Labview program, and sit on a carriage suspended over a recirculating flow tank on low-friction air bearings, allowing the entire apparatus to move upstream or downstream as the fin moves within the tank. The model fin was designed as a simplified representation of the pectoral fin of freshwater stingray *Potamotrygon orbignyi* (Castelnau 1855), as the swimming kinematics of this species have been studied in detail (Blevins and Lauder 2012). The length and width of the model fin approximate the dimensions of the pectoral fin of stingrays studied in Blevins and Lauder (2012; mean pectoral fin length ∼13 cm, mean pectoral fin width ∼6 cm). The heave, pitch and frequency values used to animate the model fin were also based on stingray data (table 1, figure 1), and created a traveling wave that passed from anterior to posterior along the fin during swimming.

Swimming performance was determined for two fins, one connected to the control apparatus by one attachment and the other by two attachments (figure 2). Both fins were attached to the motors via a metal shaft clamping the fin's leading edge; the double-attachment fin was also actuated by a second shaft, positioned two-thirds of the way along the fin. This second attachment produced a traveling wave with higher amplitude than the wave produced on the single-attachment fin, by constraining the motion of the posterior portion of the double-attachment fin. The swimming performance of single-attachment fins was determined at heave values of ±1 cm and ±2 cm, at frequencies of 1 Hz and 2 Hz (table 1). The double-attachment fin was also tested at 1 Hz and 2 Hz, with a leading edge heave of ±1 cm and posterior heave of ±2 cm (table 1). For both fins, all heave motions were accompanied by a ±20° pitch, to turn the leading edge of the fin toward the direction of heave motion, producing a more fluid, fish-like undulation. To create a smooth traveling wave along the double-attachment fin, a phase offset of 180° separated the heave and pitch of the anterior and posterior attachments.

The swimming performance of each combination of fin, frequency, and heave was compared between fins swimming in two positions: (1) the center of the recirculating flow tank ('center position') and (2) near the side wall of the tank ('wall position'). As the tank wall is perpendicular to the direction of undulation (figure 2), fins swimming near the wall experience ground effects similar to stingrays, flatfish, and similar undulatory swimmers moving near a solid substrate; 'wall effect' and 'ground effect' are interchangeable here. Fins swimming in the center of the tank were always more than 9 cm from the tank wall, yielding a gap/span ratio of ⩾1.5 (negligible ground effect; table 1). When swimming in the wall position, the posterior margin of the fin approached within 1 cm of the tank wall (0.9 cm); anterior portions of

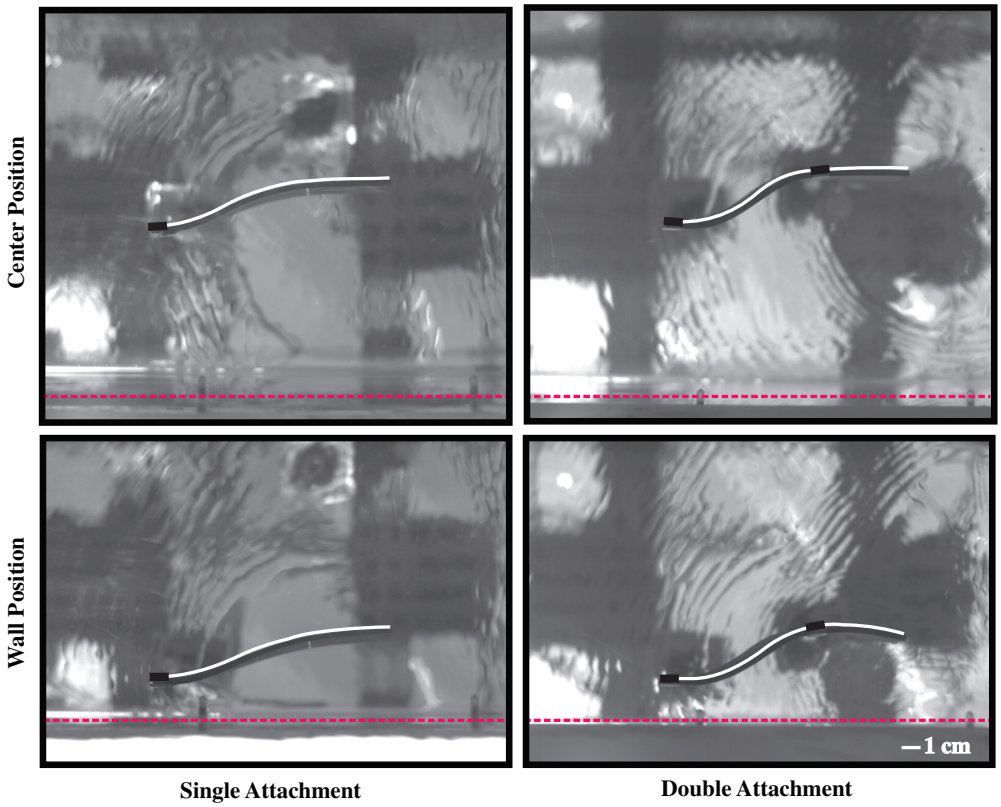

Figure 2. Ventral-view images of the single-attachment model fin (left column) and double-attachment model fin (right column) swimming at self-propelled speeds in the center of the recirculating flow tank (upper row; 'center' position) and near the tank wall (lower row; 'ground' position). Flow travels from left to right. Fins are actuated at 2 Hz and ±1 cm anterior heave (for the double-attachment fin, posterior heave = ±2 cm). Fin outlines are traced in white, with black bars indicating points of attachment to the robotic controller located above the tank. Dashed red lines near the bottom of each image highlight the position of the tank wall.

the fin undulated with slightly lower amplitude, and reached a minimum of 1.5 cm from the tank wall. The exact distance values given are for the single-attachment fin, swimming at 1 Hz and ±2 cm heave, but are representative of all conditions (figure 3). Fins in the wall position swam with a gap/span ratio of $\leqslant$0.5 (within anticipated ground effect; table 1).

Fins' swimming performance was quantified using three metrics: self-propelled swimming speed (SPS), total work, and cost of transport. The SPS of each fin was determined by matching the flow speed of the recirculating tank to the thrust produced by the moving fin, following the procedures described in previous work with the same robotic apparatus (Lauder *et al* 2007, 2011a, 2011b). In brief, linear encoders on the robotic carriage precisely track the position of the fin while the flow speed of the recirculating tank is varied. If the fin swims faster than the flow speed, it moves upstream; if it swims more slowly, it is pushed downstream. When the fin maintains an equilibrium position, thrust and drag are balanced during each cycle of motion. Rotary encoders on the recirculating tank determine the flow speed at which the fin maintains its equilibrium position; this speed is defined as the SPS of the fin under the tested swimming conditions (frequency, heave, and distance-from-ground). The mean SPS for each swimming condition was determined as the average of multiple trials (n = 15 for single-attachment fin, n = 10 for double-attachment fin).

After self-propelled speeds were determined for each swimming condition, force data were collected for single-attachment fins swimming at SPS. An ATI Nano-17 six-axis force/torque sensor (ATI Inc., Apex, North Carolina) was attached to the leading-edge shaft, simultaneously collecting three force and three torque measurements in an *XYZ* coordinate plane. Sensor tolerance did not permit force data to be collected from the double-attachment fin. A Labview trigger pulse synchronized the data collection (500 Hz) of the fin's heave position, force and torque magnitudes, and video frames from a ventral high-speed camera (FASTCAM 1024 PCI, Photron USA, Inc, San Diego, CA, USA). We used the *X* axis (upstream/downstream) forces, *Y* axis (lateral) forces, and *Z* axis (vertical) torques to calculate the fin's total work per cycle (mJ/cycle) in LabChart 7 (ADInstruments, Inc., Colorado Springs, Colorado), determining a mean total work for each swimming condition (n = 6) as the product of the combined magnitude of the forces and torques mentioned above and the distance traveled during one cycle, in terms of the SPS and any variation in upstream–downstream fin position recorded by the linear encoder. The frequency (f) and SPS for each condition were used to convert total work (W) into cost of transport (COT, in mJ m^{-1}), the energy required to travel 1 m:

$$\mathrm{COT} = \frac{W \times f}{\mathrm{SPS}}. \quad (1)$$

For each performance variable (SPS, total work, and cost of transport) a nested analysis of variance (ANOVA) with post-hoc Tukey tests was performed to determine differences

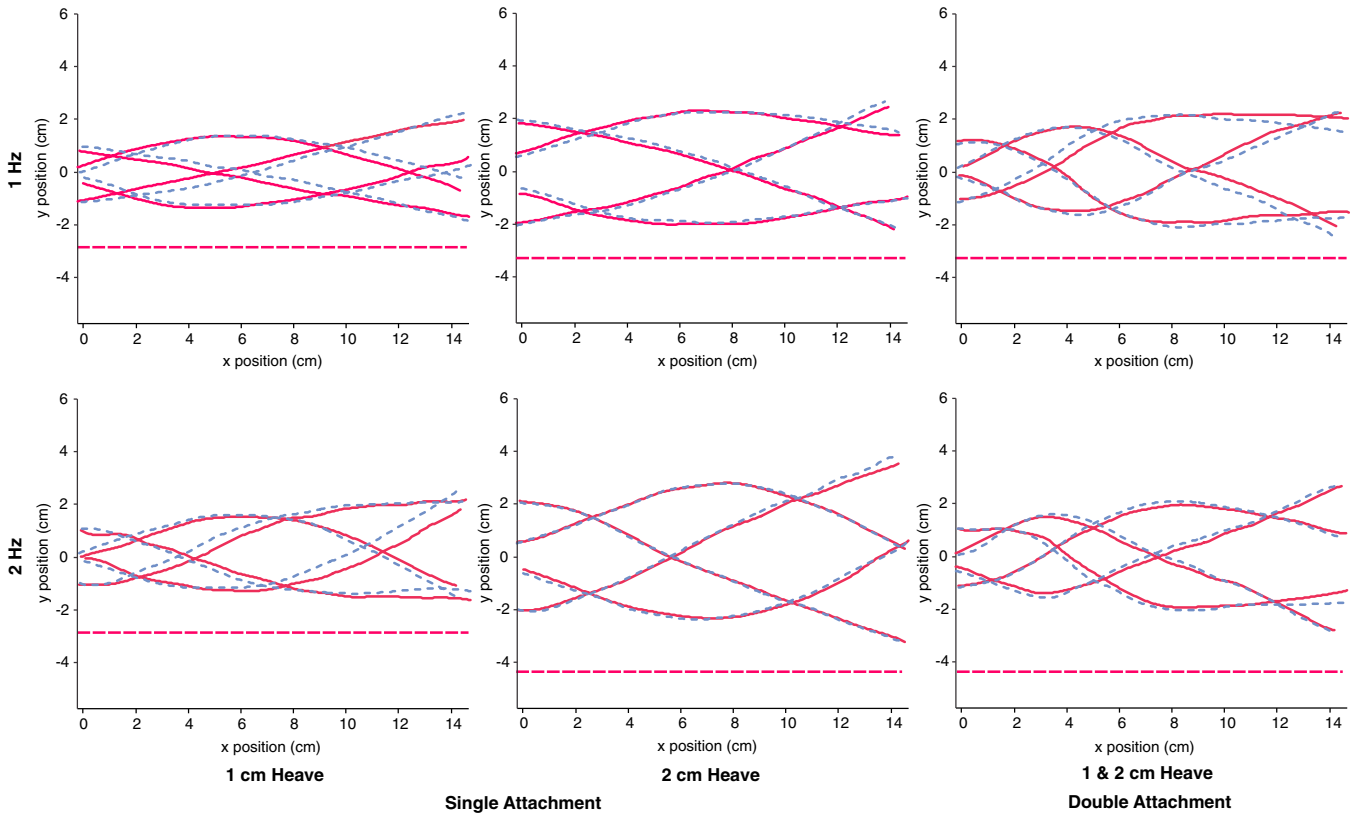

Figure 3. Midline traces through time for single- and double-attachment fins swimming at center (dashed blue lines) and wall (solid red lines) positions. Flow travels from left to right. For each condition, traces are shown for 25%, 50%, 75% and 100% of one heave cycle. Dashed red lines near the bottom of each image indicate the position of the wall for fins swimming in the wall position. For center swimming positions, the wall lies below the horizontal axis.

between center and ground swimming positions, and among swimming kinematics. Values are presented as mean ± 1 standard error.

Video footage from the ventral-view camera mentioned above was used to perform a kinematic analysis of single- and double-attachment fin motion under each swimming condition, for fins swimming at self-propelled speeds. Video of the single-attachment fin was collected synchronously with force data. All videos were viewed in Photron Motion Player 1.2.0.0 (Photron, Inc, USA), and midline positions were tracked through time using a custom program in MATLAB version 7.10 (Mathworks, Natick, MA, USA). The phase velocity of the undulatory wave (c) was calculated for each swimming condition by measuring the distance traveled by the wave crest during a known time interval. To calculate c/U, an important parameter for predicting flow patterns around a waving structure (Shen *et al* 2003), c was divided by SPS (identical to U, flow velocity). Paired t-tests were used to determine significant differences in wavespeed between center and wall positions. Gap/span ratios were calculated for all swimming conditions; as the influence of ground effect decreases as gap/span increases (Reid 1932, Rayner 1991), this verified that fins in 'wall' and 'center' positions were swimming in and out of significant ground effect regions, respectively. For undulating fins, the gap/span ratio varies during swimming as fins move toward and away from the wall. Span remains constant, as the width of the fin (7.5 cm) is the same for all conditions. To account for the variation in gap as the fin moves, an average gap was calculated by adapting the method of Webb (1993), by locating the point on the fin that approaches the wall most closely (here, the posterior margin of the fin) and determining its minimum and maximum distance from the wall during one motion cycle. The mean of these two values represented an average gap, and was divided by the constant fin span to calculate the gap/span ratio for fins swimming at center and wall positions under each kinematic condition.

Digital particle image velocimetry (DPIV) was used to visualize fluid flow around the fin. The recirculating tank was seeded with reflective particles (50 m), which were filmed by the ventral camera (same as described above) as they passed through a laser sheet generated by a continuous 10 W Coherent argon-ion laser. The laser sheet was positioned at $\frac{1}{2}$ fin height, and captured flow motion along the fin, in its wake, and between the fin and the tank wall (i.e., between fin and ground). During DPIV sequences, the fin was positioned slightly further from the tank wall than in experiments used to determine SPS and collect force data. In the near-wall position, the posterior margin of the single-attachment fin at 1 Hz and ± 2 cm heave amplitude approached within 2 cm of the tank wall, and anterior portions came within 2.5 cm, a 1 cm increase compared to the positions used in our other experiments. Lastly, DPIV sequences were recorded with no fin present in the tank, to determine the flow profile of the boundary layer near the tank wall. DPIV analyses were performed in DaVis 7.2 (LaVision Inc., Goettingen, Germany) to quantify

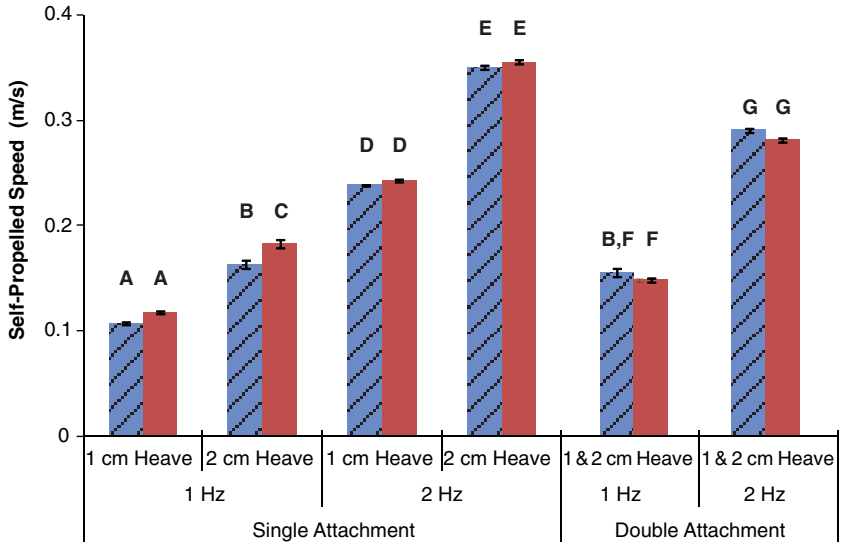

Figure 4. The self-propelled speed (m s^{-1}) of single- and double-attachment fins swimming at center (blue with hash marks) and ground (red) positions, at the given frequencies and heave amplitudes. Error bars represent ±1 standard error. Levels indicated by different letters are significantly different (nested ANOVA with Tukey post-hoc, $p < 0.01$).

velocity vectors and vorticity. In particular, the mean strength of leading-edge vortices ($n = 15$ vectors) was compared for fins swimming in center and wall positions using a Student's test, as was the average magnitude and angle of flow between the fin and wall ($n = 36$ vectors). Values are presented as mean ±1 standard error.

3. Results

3.1. Kinematics of self-propelling fins

The shape of fins during swimming varied with frequency, heave amplitude, and between single- and double-attachment fins, but showed very little change between center and wall positions (figure 3). Gap/span ratios were approximately 0.5 for fins swimming near the wall, and ⩾1.5 for fins swimming in the center of the tank (table 1). For all single-attachment conditions, approximately 0.5 waves were present on the fin at one time. Wave number was slightly higher for double-attachment fins (0.6–0.8), as was fin curvature. Under all conditions, amplitude increased by roughly one centimeter from anterior to posterior along the fin—a 50% increase for fins swimming with a ±1 cm heave, and a 25% increase for fins with ±2 cm heave. However, amplitude reached a maximum at a more anterior position on double-attachment fins than on single-attachment fins with the same anterior heave (±1 cm). This is due to the prescribed motion of the posterior attachment point (±2 cm heave) on the double-attachment fin.

Under all conditions, a traveling wave moved down the fin during swimming at self-propelled speeds. Wavespeed c increased with frequency and heave amplitude (table 1), but did not differ significantly between center and wall positions (paired t-test, $p > 0.1$). Average slip was 0.6, yielding a c/U ratio of 1.7. This indicates relatively little flow separation from the undulating fin (Shen *et al* 2003). Wavespeed and c/U values for the model fin were generally similar to those found for pectoral fin undulation during swimming by stingray *P. orbignyi* (table 1; Blevins and Lauder 2012).

3.2. Swimming performance

For most kinematics, swimming near the wall had no significant effect on the self-propelled swimming speed (SPS) of single- or double-attachment fins (figure 4; nested ANOVA, Tukey post-hoc, $p > 0.05$). Only the single-attachment fin swimming at 1 Hz with a 2 cm heave showed a significant change in SPS near the wall, swimming 13 ± 1% (mean ±1 standard error) faster than in the center of the tank (Tukey post-hoc, $p < 0.0001$); the trend toward increased SPS near the wall was non-significant for the remaining single-attachment fin conditions. For double-attachment fins, there was a slight trend toward decreased swimming speed near the wall. Predictably, SPS increased with both frequency and heave amplitude across kinematic groups (nested ANOVA, $p < 0.0001$, Tukey post-hoc, $p < 0.0001$).

For the single-attachment fin, total work increased significantly when fins swam near the wall, under all kinematic conditions (figure 5; nested ANOVA, Tukey post-hoc, $p < 0.02$). In general, the magnitude of the effect increased slightly across kinematic groups, ranging from 0.9 ± 0.2 mJ/cycle (mean ±1 standard error) under the 1 Hz 1 cm condition to 1.3 ± 0.3 mJ/cycle under the 1 Hz 2 cm condition and 1.7 ± 0.4 mJ/cycle for fins swimming at 2 Hz 2 cm; however, the 2 Hz 1 cm condition had the lowest effect magnitude at 0.6 ± 0.4 mJ/cycle. Relative effect size—the percent change in total work between center and wall positions for a given set of kinematics—was greatest for fins moving at lower frequencies and (for the 1 Hz condition) heave amplitudes. For fins swimming at 1 Hz, total work increased near the wall by 21 ± 6% for a 1 cm heave amplitude and 12 ± 3% with a 2 cm amplitude. Fins swimming at 2 Hz experienced a 4 ± 1% and 5 ± 1% increase in total work near the wall for 1 and 2 cm heave amplitudes, respectively. Total work also increased with frequency and heave amplitude, across kinematic groups (nested ANOVA, Tukey post-hoc, $p < 0.0001$).

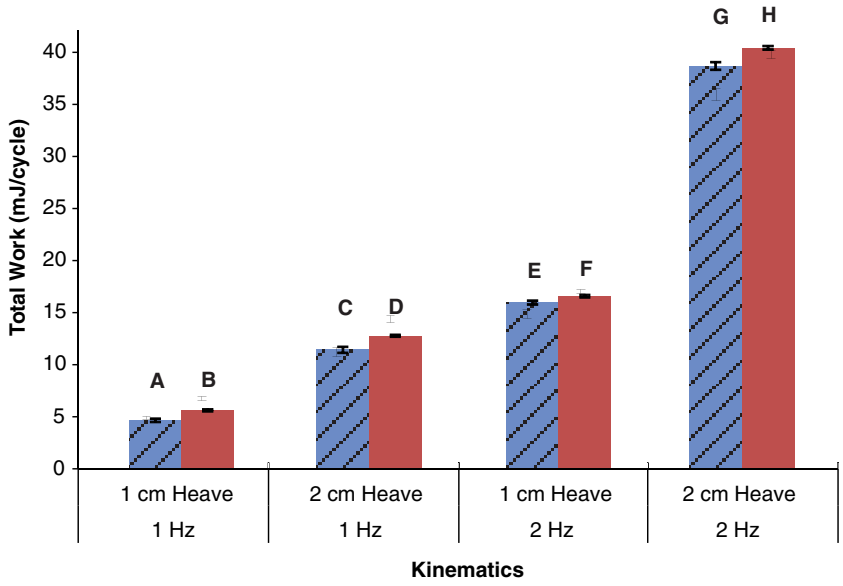

Figure 5. Total work per cycle (mJ/cycle) for each single-attachment fin condition, at center (blue with hash marks) and ground (red) positions at the given frequencies and heave amplitudes. Error bars represent ±1 standard error. Levels indicated by different letters are significantly different (nested ANOVA with Tukey post-hoc, $p < 0.0001$ for kinematic comparisons, $p < 0.02$ for position comparisons).

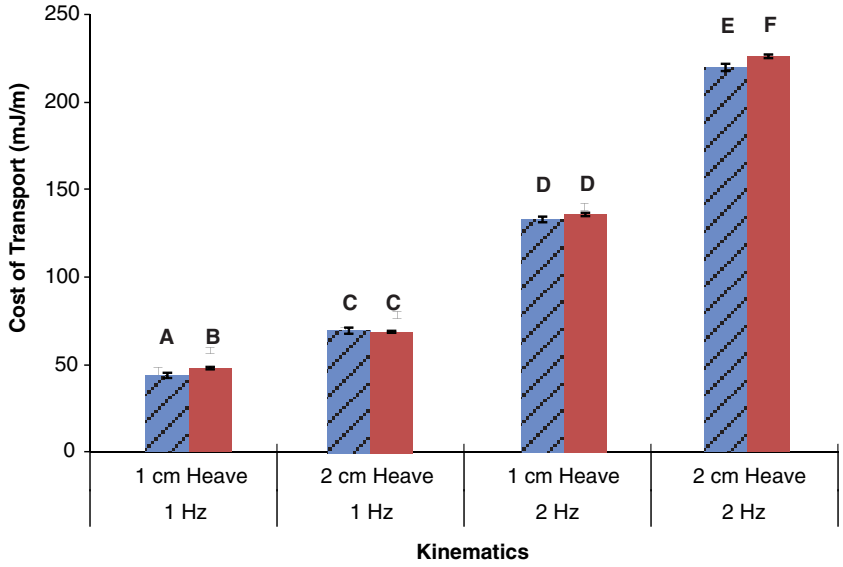

Figure 6. Cost of transport (mJ m^{-1}) for each single-attachment fin condition, at center (blue with hash marks) and ground (red) positions at the given frequencies and heave amplitudes. Cost of transport is calculated from total work using swimming frequency and self-propelled speed. Error bars represent ±1 standard error. Levels indicated by different letters are significantly different (nested ANOVA with Tukey post-hoc, $p < 0.0001$ for kinematic comparisons, $p < 0.04$ for position comparisons).

Cost of transport increased when fins swam near the wall under some kinematic conditions, but remained constant under others (figure 6). Fins with identical swimming kinematics had significantly higher costs of transport near the wall than in the center of the tank (nested ANOVA, Tukey post-hoc, $p < 0.04$), when swimming at 1 Hz 1 cm and 2 Hz 2 cm; cost of transport did not differ between center and wall positions for the 1 Hz 2 cm and 2 Hz 1 cm conditions (Tukey post-hoc, $p > 0.05$). For the 1 Hz 2 cm condition, the increase in total work for near-wall swimming was counterbalanced by increased SPS near the wall, reducing the effect on cost of transport. For the 2 Hz 1 cm condition, the increase in total work was significant but quite small, resulting in a non-significant change in cost of transport for these kinematics. For the kinematic conditions showing significant effects, cost of transport increased near the wall by 4.1 ± 2.1 mJ m^{-1} for the 1 Hz 1 cm condition and 6.4 ± 2.4 mJ m^{-1} for the 2 Hz 2 cm condition. Therefore, similar to the results for total work, relative effect size decreased as swimming frequency and heave amplitude increased: near the wall, cost of transport increased by 27 ± 5% for the 1 Hz 1 cm condition, 14 ± 2% for 1 Hz 2 cm (not significant), 13 ± 4% for 2 Hz 1 cm, and 9 ± 1% for 2 Hz 2 cm. Cost of transport also increased across kinematic groups with frequency and heave amplitude (nested ANOVA, Tukey post-hoc, $p < 0.0001$).

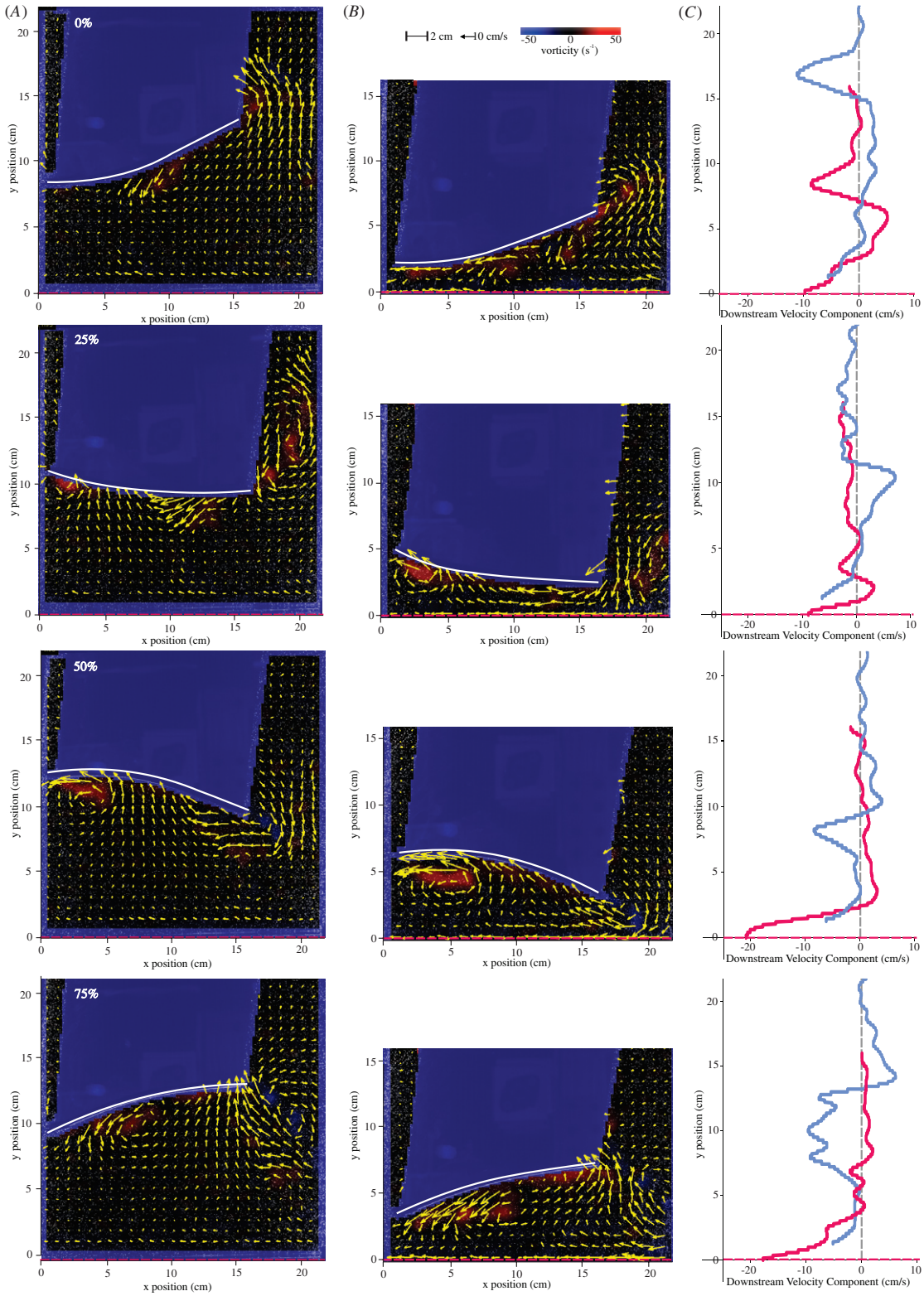

Figure 7. Hydrodynamic analysis of flow around fins swimming in center (*A*) and ground (*B*) positions in a recirculating flow tank, with comparison of wake profiles between the two positions (*C*). From top to bottom, images illustrate flow at 25% intervals through one motion cycle (125 ms between images), beginning when the leading edge of the fin is closest to the ground (dashed red line). Fins (highlighted in white) are swimming at 1 Hz, ±2 cm heave amplitude, at their self-propelled speeds. Yellow vector arrows represent flow speed and direction relative to freestream flow, with vorticity indicated by red (positive) and blue (negative) shading. For clarity, only 1/4 of vectors are shown. Vectors were not computed for masked areas (bright blue) behind the fin and overlapping the ground; masked areas and ground positions appear slightly different between (*A*) and (*B*) due to the different camera positions required to film fins in the center of the tank and near the ground. Flow profiles (*C*) show the downstream component of velocity vectors at a transect across the fin's wake, 2 cm downstream of the trailing edge of the fin (parallel to the *y*-axis in (*A*) and (*B*)). Profiles were determined for fins swimming in center (blue) and ground (red) positions, and are shown relative to a reference line at zero (gray dashed line); timesteps correspond to (*A*) and (*B*). See online publication for color images.

3.3. Hydrodynamics

Particle image velocimetry reveals differences in flow patterns around fins swimming in the center of the tank and near the tank wall (figure 7). Hydrodynamic data are presented for fins swimming at 1 Hz 2 cm, as these kinematics produce the largest position-dependent change in self-propelled speed, and show increases in total work and cost-of-transport similar to other kinematic conditions; the 1 Hz 2 cm condition therefore offers the best insight into the hydrodynamics of ground effect. For fins near and far from the wall, flow is dominated by a strong leading-edge vortex, which detaches from the leading edge and propagates along the length of the fin until it is shed. As fins undulate toward and away from the wall, leading-edge vortices develop on alternate sides of the fin. Vortices occurring on the side of the fin closer to the wall were analyzed to investigate alterations in flow due to ground effects. For fins swimming near the wall and in the center of the tank, these vortices reached maximum rotational strength (vorticity) at 50% of the fin cycle, as the leading edge of the fin reached its maximum heave distance from the wall and began to return towards the wall (figures 7(*A*), (*B*)). Maximum vortex strength was significantly higher for fins swimming near the wall, with maximum rotation values of 41.4 $\pm$ 2.6 s^{-1} near the wall versus 32.4 $\pm$ 3.2 s^{-1} in the center of the tank (Student's *t*-test, $p < 0.05$). The second key difference in the hydrodynamics of fins swimming near and far from the wall involves the direction of fluid jets shed from the fin. As the leading edge of the fin begins to move away from the wall, the posterior portion of the fin continues toward the wall, making its closest approach (25% cycle, figures 7(*A*), (*B*)). At this point in the cycle, fins shed a jet of fluid; for fins swimming near the wall, this jet enters the narrow gap between fin and wall. The magnitude of the jet was not significantly different between center and wall swimming positions (16.1 $\pm$ 1 cm and 15.6 $\pm$ 1 cm, respectively, $p > 0.05$). However, when fins swim near the wall, the jet is oriented almost directly upstream (5.6 $\pm$ 0.1° from the horizontal), while fins swimming in the center of the tank produce a more laterally oriented jet (33.6 $\pm$ 0.1°) (Student's *t*-test, $p < 0.05$).

Wake profiles of streamwise velocity also reveal differences in wake structure for fins swimming in center and near-wall positions, throughout the motion cycle (figure 7(*C*)). During the second half of the cycle, as fins' leading edge moved toward the wall, the wake profile of fins swimming far from the wall shows large regions of negative flow (−10 cm s^{-1}) relative to freestream velocity. At the same time, wake profiles of fins swimming near the wall show relative velocities near zero, except for a region of negative velocity adjacent to the wall, within the boundary layer measured for our recirculating tank. As the fin approaches the wall, the boundary layer thins as it is disrupted by orthogonal, fin-related flows.

4. Discussion

Undulating fins swimming near a solid boundary experience a fundamentally different fluid regime than when swimming in effectively unbounded fluid. Ground effect decreases non-monotonically with distance from the substrate, falling to zero at a gap/span ratio of 3 (for fixed, non-undulating propulsors; Reid 1932, Blake 1979, 1983) but substantially reduced even at a ratio of 1 (<10% effect, Webb 1993). In this study, fins swimming near the wall swam with a gap/span ratio of approximately 0.5, well within ground-effect range (table 1). In contrast, fins far from the wall swam with a gap/span ratio greater than 1.5, indicating negligible ground effect. Therefore, comparisons of swimming performance between the two positions will demonstrate the consequences of undulating near a solid boundary.

Our model system allows consistent kinematic inputs (frequency and heave amplitude) for fins swimming in and out of ground effect, in contrast to experiments conducted with live animals, which change their behavior when swimming close to a solid boundary (Webb 1993, 2002). The motion of fins' leading edge is proscribed (and, for double attachment fins, so is the motion of the second attachment point at 2/3 fin-length), but proximity to the wall could still skew overall kinematics by altering the motion of the passive portion of the fin, changing the amplitude of its posterior edge, the symmetry of fin excursions, etc. However, kinematic analyses reveal no substantial alterations in fins' midline motion due to ground effect, under any kinematic condition; fin motion is the same near and far from the wall (figure 3). Subtle influences of ground effect on fin shape may not be visible here due to the stiffness of the model fin, which might resist deformation due to ground effect forces. The fin material was selected to produce traveling waves of undulation during swimming, but could not be matched to biological systems as the *in vivo* stiffness of swimming fish is unknown (McHenry *et al* 1995, Lauder *et al* 2011a). (The influence of material stiffness on the kinematics of similar model fins has been examined in Alben *et al* 2012, but is beyond the scope of this study.) Yet, if a sparsely actuated, flexible foil resists passive deformations due to ground effect, it seems likely that the kinematic changes observed in fish swimming in ground effect are due to active modulation, not passive effects.

Fins undulating near the wall can have significantly different swimming performance compared to identical fins swimming at identical frequencies and heave amplitudes far from the wall. Contrary to the findings for models of fixed-wing foils (Baudinette and Schmidt-Nielsen 1974, Withers and Timko 1977, Hainsworth 1988, Blake 1979, Park and Choi 2010) and heaving foils (Tanida 2001, Molina and Zhang 2011), the undulating fins tested here did not experience performance gains from ground effect. For most kinematic conditions, fins did not swim significantly faster near the wall (figure 4), and in all cases significantly more power was required per cycle (figure 5). Therefore, swimming near the wall incurred a cost of transport higher than or equal to the cost of swimming far from the wall (figure 6). Ground effect 'penalties' to cost of transport varied with kinematics, ranging up to 10%; increases in cost of transport on this scale are meaningful for both organisms and artificial devices.

However, small changes in kinematics can alter performance outcomes. A statistically-significant increase in self-propelled swimming speed near the wall occurred for only one kinematic condition (single-attachment, 1 Hz $\pm$2 cm

heave condition; figure 4). Total work also increased in this position (figure 5), but the combination yielded the same cost of transport for fins near and far from the wall, rather than the increased cost of transport seen near the wall under all other conditions (figure 6). So for certain kinematics, an undulating fin can swim at higher velocities in ground effect without losing efficiency relative to its cost-of-transport out of ground effect. Overall trends in self-propelled speed near and far from the wall also vary with kinematics (figure 4). Single-attachment fins swimming at 1 Hz swam ∼10% faster near the wall, for both 1 and 2 cm heave values. In contrast, the trend for single-attachment fins swimming at 2 Hz was negligible, with differences an order of magnitude below those found for 1 Hz, and swimming speed *decreased* (by ∼4%) for double attachment fins swimming near the wall, at both frequencies. Though the effects here are slight, we see that the same fin can experience different—and even opposite—ground effects, depending on kinematics. This suggests that the kinematic changes observed in fish swimming in ground effect (reduced tailbeat frequency and amplitude; Webb 1993, 2002) may be a mechanism for transforming potential locomotor penalties into performance benefits. Stingrays have extremely fine control of pectoral fin conformation (Blevins and Lauder 2012), with the potential for precise kinematic tuning to exploit ground effect.

Kinematics influence ground effect because they determine the effective shape of a moving foil. Small changes in ground effect outcomes are seen over the range of frequencies and amplitudes tested here, but the overall ground effects on any of the undulating fins in this study differ from what fixed foils experience, because the effective shape of moving foils constantly changes through time. Shape (e.g. camber, angle of attack) makes a profound difference in the influence of ground effect on fixed-wing foils, in combination with their distance from the substrate. Under some conditions, ground effects on fixed-wing foils increase lift and reduce drag (e.g. Ahmed and Sharma 2005). In other cases drag is reduced but lift is unchanged (e.g. Withers and Timko 1977, Zhang *et al* 2004), or lift may even become negative and accompanied by increased drag (Zerihan and Zhang 2000). Drag effects are determined by the interaction of shed vortices with the substrate, which can alter wake structure, while lift outcomes depend on the pressure changes induced between the foil and the ground. If local pressure decreases, downforce (negative lift) increases due to suction forces (Vogel 1994, Zerihan and Zhang 2000). Race cars use this type of ground effect to keep fast-moving vehicles engaged with the road (Jones and Smith 2003, Katz 2006). In the lift-enhancing case, flow is compressed between the foil and the ground; local pressure is increased, and so is lift (Vogel 1994, Ahmed and Sharma 2005). Fish-like undulating foils will transition between positive and negative lift states, as effective camber, angle of attack, and direction of motion change during the heave cycle. In addition, ground effects depend not only on the current shape of the foil, but its previous conformation. Molina and Zhang (2011) note hysteresis in the forces experienced by a heaving foil in ground effect; undulating fins are subject to the same effect, as the flows shaped by the foil at one point in time determine the forces acting upon the foil at later points in time.

A description of flow around undulating fins in ground effect is presented here (figure 7) in order to help explain the increased cost of transport observed for undulating fins near the wall. By comparing the hydrodynamics of identical fins with consistent kinematics swimming in freestream and near-wall positions, differences due to the influence of the ground can be detected. As the leading edge of the fin moves away from the wall during the first half of the motion cycle, flow around fins both near and far from the wall is dominated by a strong leading edge vortex, developed on the side of the fin closer to the wall (figures 7(*A*), (*B*)). Vortices create areas of low pressure, inducing suction; due to the fin's orientation as the leading edge vortex forms, a component of the suction force vector aligns with the fin's direction of travel, and the fin is 'pulled' forward (Wolfgang *et al* 1999). Fins undulating near the wall develop stronger ground-side leading edge vortices than freestream fins (41.4 ± 2.6 versus 32.4 ± 3.2 s^{-1}, $p < 0.05$). Therefore, fins swimming near the wall will also experience stronger suction forces.

As the fin's leading edge moves away from the wall during the first half of the motion cycle, the posterior portion of the fin continues toward the wall (figures 7(*A*), (*B*)), shedding a jet of fluid. For fins swimming in ground effect, the presence of the nearby wall alters the orientation of this jet to face almost directly upstream ($5.6 \pm 0.1^\circ$ from the horizontal), significantly different from the more lateral jet shed by fins swimming far from the wall ($33.6 \pm 0.1^\circ$ from the horizontal; $p < 0.05$). The magnitude of fluid flow does not differ significantly between these two states ($p > 0.05$). Therefore, fins swimming in ground effect may experience a locomotor benefit from the 'cushion' of fluid moving between fin and wall, along the same vector as the fin's direction of travel—this effect may be responsible for the increase in self-propelled speed determined for this swimming condition.

Flow compression due to the nearby wall also occurs during the second half of fins' motion cycle, as the leading edge of the fin moves toward the wall (figures 7(*B*), (*C*)), similar to predictions by Argentina *et al* (2007). In particular, the leading-edge vortex developed on the side of the fin closer to the wall during the first half of the cycle is compressed as the fin moves back toward the wall. In the freestream case there can be no compression. In air, fluid compression effects could potentially allow a thin, undulating foil to fly, hovering over a solid substrate on a high-pressure fluid cushion (Argentina *et al* 2007). Neither the model fin tested here nor live stingrays depend on this effect to suspend themselves in the water column, as they are well capable of swimming far from the substrate. However, just as reduced pressure due to the leading edge vortex can act to pull the fin forward, increased pressure between the wall and the posterior portion of the fin due to flow compression may increase lift. Lift effects depend on the fin's effective angle of attack, as it changes direction and begins to move away from the wall. The increased power requirements (and cost of transport) for swimming near the wall may occur as fins must overcome fluid forces to continue moving toward the wall despite high-pressure areas of flow compression beneath the fin, or away from the wall despite low-pressure regions between fin and ground.

Locomotion near a solid boundary inevitably involves the boundary layer, the velocity gradient that surrounds solid objects in moving fluid, with flow velocity decreasing to zero at the boundary (Vogel 1994). A relatively undisturbed boundary layer is present when fins are at their maximum distance from the wall, but as fins approach the wall the boundary layer is disturbed and virtually disappears (figure 7(*C*)). Therefore, performance effects are not simply due to swimming in a low-flow region, but result from changes in fluid pressure and direction induced by fin motion.

In this paper a simple model system is used to offer an experimental analysis of the interaction of an undulating fin and ground effect, and reveals that locomotion near the substrate can have significant impacts on swimming performance. The dynamic ground effects experienced by undulating fins differ from fixed-wing ground effects, as fins' effective shape and distance from the substrate changes through time. Rather than the performance gains observed for fixed-wing systems in ground effect (Baudinette and Schmidt-Nielsen 1974, Withers and Timko 1977, Hainsworth 1988, Rozhdestvendky 2006, Park and Choi 2010), the undulating fins examined here generally incur costs from moving close to a solid boundary. However, ground effect outcomes depend on swimming kinematics. The waveforms produced by undulating model fins (table 1; figure 3) are similar in amplitude and wavespeed to the pectoral fin waveforms used by freshwater stingray *Potamotrygon orbignyi* (table 1; figure 1(*B*)), and similar flow patterns are observed for model fins and stingray fins undulating near the substrate, with vortices trapped and compressed beneath the fin (figures 1(*C*), 7(*A*), (*B*)). However, the broad, flexible fins of stingrays allow fine control of fin conformation during locomotion (Schaefer and Summers 2005, Blevins and Lauder 2012). Small alterations in three-dimensional fin shape may allow these benthic swimmers to modulate near-substrate flow and avoid the costs of undulating in ground effect experienced by model fins. The kinematic changes seen in plaice during near-ground locomotion may serve the same purpose (Webb 2002). Otherwise, while the presence of a nearby substrate can enhance crypsis or foraging, benthic undulatory swimmers may incur substantial costs to swimming performance by swimming near the ground. Robotic models provide an excellent platform for further investigations of dynamic ground effects on moving fins, wings, and limbs, to better understand the locomotor environment of benthic animals and inform the design of biomimetic systems.

Acknowledgments

We thank Erik Anderson, Vernon Baker, Ryan Shelton and Chuck Witt for their work on the design and control of the robotic apparatus and associated programs. We are particularly grateful for the support and advice of Jeanette Lim, Brooke Flammang-Lockyer, and other members of the Lauder Lab. This research was supported by NSF grant EFRI-0938043 to George V Lauder, and support from the Harvard University Department of Organismic and Evolutionary Biology.

References

Ahmed M R and Sharma S D 2005 An investigation on the aerodynamics of a symmetrical airfoil in ground effect *Exp. Therm. Fluid Sci.* **29** 633–47

Alben S, Witt C, Baker T V, Anderson E and Lauder G V 2012 Dynamics of freely swimming flexible foils *Phy. Fluids* **24** 051901

Argentina M, Skotheim J and Mahadevan L 2007 Settling and swimming of flexible fluid-lubricated foils *Phys. Rev. Lett.* **99** 224503

Baudinette R V and Schmidt-Nielsen K 1974 Energy cost of gliding flight in herring gulls *Nature* **248** 83–4

Blake R W 1979 The energetics of hovering in the mandarin fish (*Synchropus picturatus*) *J. Exp. Biol.* **82** 25–33

Blake R W 1983 Mechanics of gliding birds with special reference to the influence of ground effect *J. Biomech.* **16** 649–54

Blevins E and Lauder G V 2012 Rajiform locomotion: three-dimensional kinematics of the pectoral fin surface during swimming by freshwater stingray *Potamotrygon orbignyi J. Exp. Biol.* **215** 3231–41

Goto T, Nishida K and Nakaya K 1999 Internal morphology and function of paired fins in the epaulette shark, *Hemiscyllium ocellatum Ichthyol. Res* **46** 281–7

Hainsworth F R 1988 Induced drag savings from ground effect and formation flight in brown pelicans *J. Exp. Biol.* **135** 431–44

Jones M A and Smith F T 2003 Fluid motion for car undertrays in ground effect *J. Eng. Math.* **45** 309–34

Katz J 2006 Aerodynamics of race cars *Annu. Rev. Fluid Mech.* **38** 27–63

King H M, Shubin N H, Coates M I and Hale M E 2011 Behavioral evidence for the evolution of walking and bounding before terrestriality in sarcopterygian fishes *Proc. Natl Acad. Sci. USA* **52** 21146–51

Koester D M and Spirito C P 2003 Punting: an unusual mode of locomotion in the Little Skate, *Leucoraja erinacea* (Chondrichthyes: Rajidae) *Copeia* **3** 553–61

Lauder G, Tangorra J, Lim J, Shelton R, Witt C and Anderson E J 2011a Robotic models for studying undulatory locomotion in fishes *Mar. Technol. Soc J.* **45** 41–55

Lauder G V, Anderson E J, Tangorra J and Madden P G A 2007 Fish biorobotics: kinematics and hydrodynamics of self-propulsion *J. Exp. Biol.* **210** 2767–80

Lauder G V, Madden P G A, Tangorra J, Anderson E and Baker T V 2011b Bioinspiration from fish for smart material design and function *Smart Mater. Struct.* **20** 09401

Lucifora L O and Vassallo A I 2002 Walking in skates (Chondrichthyes. Rajidae): anatomy, behaviour and analogies to tetrapod locomotion *Biol. J. Linn. Soc.* **77** 35–41

Macesic L J and Kajiura S M 2010 Comparative punting kinematics and pelvic finmusculature of benthic batoids *J. Morph.* **271** 1219–1228

McHenry M J, Pell C A and Long J A 1995 Mechanical control of swimming speed: stiffness and axial wave form in undulating fish models *J. Exp. Biol.* **198** 2293–305

Molina J and Zhang X 2011 Aerodynamics of a heaving airfoil in ground effect *AIAA J.* **49** 1168–79

Nowroozi B N, Strother J A and Horton J M 2009 Whole-body lift and ground effect during pectoral fin locomotion in the northern spearnose poacher (*Agonopsis vulsa*) *Zoology* **112** 393–402

Park H and Choi H 2010 Aerodynamic characteristics of flying fish in gliding flight *J. Exp. Biol.* **213** 3269–79

Pietch T W and Grobecker D B 1987 *Frogfishes of the World* (Stanford, CA: Stanford University Press)

Pridmore P A 1994 Submerged walking in the epaulette shark *Hemiscyllium ocellatum* (Hemiscyllidae) and its implications for locomotion in rhipidistian fishes and early tetrapods *Zool. Anal. Complex Syst.* **98** 278–97

Rayner J M V 1991 On the aerodynamics of animal flight *Phil. Trans. R. Soc. B.* **334** 119–28
Reid E G 1932 *Applied Wing Theory* (New York, NY: McGraw-Hill)
Renous S, Gasc J P, Bels V L and Davenport J 2000 Six-legged walking by a bottom-dwelling fish *J. Mar. Biol. Assoc. UK* **80** 757–8
Rozhdestvendky K 2006 Wing-in-ground effect vehicles *Prog. Aerosp. Sci.* **42** 211–83
Schaefer J T and Summers A P 2005 Batoid wing skeletal structure: novel morphologies, mechanical implications, and phylogenetic patterns *J. Morphol.* **264** 298–313
Shen L, Zhang X, Yue D K P and Triantafyllou M S 2003 Turbulent flow over a flexible wall undergoing a streamwise travelling wave motion *J. Fluid Mech.* **484** 197–221
Tanida Y 2001 Ground effect in flight (birds, fishes, and high-speed vehicle) *JSME Int. J. B* **44** 481–6
Tytell E D and Lauder G V 2004 The hydrodynamics of eel swimming I. Wake structure *J. Exp. Biol.* **207** 1825–41
Vogel S 1994 *Life in Moving Fluids: The Physical Biology of Flow* (Princeton, NJ: Princeton University Press)
Ward A B 2002 Kinematics of the pectoral fins in batfishes (*Ogcocephalidae*) during aquatic walking *Integr. Comp. Biol.* **6** 1331
Webb P W 1981 The effect of the bottom on the fast start of a flatfish, *Citharichthys stigmaeus Fish Bull.* **79** 271–6
Webb P W 1993 The effect of solid and porous channel walls on steady swimming of steelhead trout *Oncorhynchus mykiss J. Exp. Biol.* **178** 97–108
Webb P W 2002 Kinematics of plaice, *Pleuronectes platessa*, and cod, *Gadus morhua*, swimming near the bottom *J. Exp. Biol.* **205** 2125–34
Wilga C D and Lauder G V 2001 Functional morphology of the pectoral fins in bamboo sharks, *Chiloscyllium plagiosum*: benthic versus pelagic station-holding *J. Morphol.* **249** 195–209
Withers P C and Timko P L 1977 The significance of ground effect to the aerodynamic cost of flight and energetics of the black skimmer (*Rhyncops nigra*) *J. Exp. Biol.* **70** 13–26
Wolfgang M J, Anderson J M, Grosenbaugh M A, Yue D K P and Triantafyllou M S 1999 Near-body flow dynamics in swimming fish *J. Exp. Biol.* **202** 2303–27
Zerihan J and Zhang J 2000 Aerodynamics of a single element wing in ground effect *J. Aircr.* **37** 1058–64
Zhang X, Senior A and Ruhrmann A 2004 Vortices behind a bluff body with an upswept aft section in ground effect *Int. J. Heat Fluid Flow* **25** 1–9